

Prostate cancer magnetic resonance imaging (MRI): multidisciplinary standpoint

Liang Li¹, Liang Wang¹, Zhaoyan Feng¹, Zhiquan Hu², Guoping Wang³, Xianglin Yuan⁴, He Wang⁵, Daoyu Hu¹

¹Department of Radiology, Tongji Hospital, Tongji Medical College, Huazhong University of Science and Technology, Wuhan 430030, China;

²Department of Urology, Tongji Hospital, Tongji Medical College, Huazhong University of Science and Technology, Wuhan 430030, China;

³Institute of Pathology, Tongji Hospital, Tongji Medical College, Huazhong University of Science and Technology, Wuhan 430030, China;

⁴Department of Oncology, Tongji Hospital, Tongji Medical College, Huazhong University of Science and Technology, Wuhan 430030, China;

⁵Research Specialist GE Healthcare, ZhangJiang Hi-Tech Park, Pudong, Shanghai 201203, China

Corresponding to: Liang Wang. Department of Radiology, Tongji Hospital, Tongji Medical College, Huazhong University of Science and Technology, 1095, Jiefang Avenue, Wuhan 430030, China. Email: wangliang2001@gmail.com.

Abstract: Prostate cancer is the most common cancer diagnosed in men and a leading cause of death. Accurate assessment is a prerequisite for optimal clinical management and therapy selection of prostate cancer. There are several parameters and nomograms to differentiate between patients with clinically insignificant disease and patients in need of treatment. Magnetic resonance imaging (MRI) is a technique which provides more detailed anatomical images due to high spatial resolution, superior contrast resolution, and multiplanar capability. State-of-the-art MRI techniques, such as diffusion weighted imaging (DWI), MR spectroscopic imaging (MRSI), dynamic contrast enhanced MRI (DCE-MRI), improve interpretation of prostate cancer imaging. In this article, we review the major role of MRI in the advanced management of prostate cancer to noninvasively improve tumor staging, biologic potential, treatment planning, therapy response, local recurrence, and to guide target biopsy for clinical suspected cancer with previous negative biopsy. Finally, future challenges and opportunities in prostate cancer management in the area of functional MRI are discussed as well.

Key Words: Prostate cancer; magnetic resonance imaging; management; treatment



Submitted Feb 08, 2013. Accepted for publication Mar 12, 2013.

doi: 10.3978/j.issn.2223-4292.2013.03.03

Scan to your mobile device or view this article at: <http://www.amepc.org/qims/article/view/1815/2551>

Introduction

It was in 1853 that John Adams first described a case of prostate cancer (Pca) in a 59-year-old male patient, and this disease was considered rare because of the short life expectancy at the time. In 2012, there were expected to be about 239,000 new cases diagnosed with Pca and about 30,000 Pca deaths (1). Nowadays, it is the most common noncutaneous cancer and the second/third leading cause of cancer death in men in the United States and European Community (1-3). The management and imaging in Pca remains a big challenge.

The main diagnostic biomarker for Pca is prostate-specific antigen (PSA). PSA test was approved by the U.S. Food and Drug Administration (FDA) in 1986 to monitor the disease status (4). However, a PSA test has some drawbacks. It is not capable of differentiating between Pca, benign prostatic hyperplasia (BPH), and chronic prostatitis, particularly when serum PSA level is lower than 10 ng/mL. This method indeed produces over-diagnosis of clinically insignificant cancers. Thus, in 2012, the U.S. Preventive Services Task Force (USPSTF) recommended against PSA-based screening all men for Pca (5). Transrectal Ultrasound (TRUS)-guided prostate biopsy has become a standard method to obtain

specimen for histopathological examination. Positive results of biopsy of the prostate confirm clinical suspicion of Pca, but they provide limited information on extent and differentiation of Pca. Furthermore, prostate biopsy without evidence of Pca does not rule out its presence (6).

To replace somewhat arbitrary combinations of individual variables, there is a need for instruments to aid patients and their physicians in treatment decision. Using algorithms that incorporate multiple variables, the nomograms have been developed to give a prediction of the pathologic stage, the probability of freedom from disease recurrence. The Partin staging nomogram (also called the “Partin tables”), which is based on serum PSA value, clinical stage, Gleason score, and was first published in 1993 and was updated in 1997 and again in 2001 to predict the pathological stage at radical prostatectomy. Other nomograms, such as Kattan’s nomograms, have been developed to predict stage, recurrence, or biologic potential (7). As an important advance in accurate prediction for clinical medicine, the nomograms allow calculation of the continuous probability of a particular trend and tend to outperform both expert clinicians and risk grouping. The nomograms are widely used for individual patient counseling and important decision-making. However, the nomograms are limited by the lack of results from imaging studies and digital rectal examination (DRE)-based clinical staging. Thus, despite the high predictive ability and the cost-effectiveness of the nomograms, there is still some room for improved accuracy of prediction.

MRI is a good imaging modality of choice in Pca detection, localization, and staging (8-10). The interpretation of Pca on T2-weighted MR imaging (T2WI) can be affected by false-positive findings such as prostatitis, postbiopsy hemorrhage, and fibrosis (11,12). To improve the diagnostic accuracy of Pca imaging, functional MR imaging (fMRI) techniques have been applied, such as diffusion-weighted MR imaging (DWI) (13-15), proton (1H) MR spectroscopic imaging (MRSI) (16-18), and dynamic contrast-enhanced MR imaging (DCE-MRI) (19-21).

DWI has quickly evolved to become one of the most relevant sequences for imaging Pca. In tumor, the increased cellularity and associated loss of ductal morphology result in a smaller extracellular space, the restriction of water diffusion and a corresponding reduction in ADC values (22). A recent meta-analysis demonstrated the sensitivity and specificity of DWI combined with T2WI to range from 65% to 84% and 77% to 87%, respectively (23). MRSI identifies Pca by an increased ratio of choline plus polyamines plus

creatine to citrate (24). As a result of increased energy metabolism, the citrate level is reduced in tumor. Owing to a high phospholipid cell membrane turnover the choline level is elevated in proliferating malignant tissue (25). DCE-MR imaging relies on tumor neoangiogenesis for Pca detection. In malignant tumour, the number of vessels (microvascular density) is increased in comparison with the surrounding normal tissue, leading to greater relative tumoral enhancement (26).

This review addresses the major role of MRI in the advanced management of Pca to improve cancer staging noninvasively, biologic potential, treatment planning, therapy response, local recurrence, and to guide target biopsy for clinically suspected cancer with previous negative biopsy, and discusses the future prospects of MRI in Pca management from a multidisciplinary standpoint.

Prostate cancer staging

The staging of Pca is based on tumor, node and metastasis (TNM) staging. The latest modification was made in 2010 by the American Joint Committee on Cancer (AJCC). The 2010 revised TNM system, shown in *Table 1*, is clinically useful and precisely stratifies newly diagnosed cancer (27). The most important advantage is distinguishing between patients with pathologically organ-confined Pca (pT2) from those with non-confined Pca (pT3-4). As is well known, once the tumor extends outside the prostate, the chances of cure are substantially diminished (28,29).

Detection of OCPC (pT2)

Clinicians must distinguish between patients with pathologically organ-confined prostate cancer (OCPC) (pT2) and those with non-organ-confined prostate cancer (pT3-4). T2 tumors are subclassified as T2a (less than one-half of one lobe involved) (*Figure 1*), T2b (more than one-half of one lobe involved), and T2c (bilateral involvement). After radical prostatectomy (RP), patients with OCPC have an excellent prognosis, as more than 90% of them are free from biochemical recurrence in the period of 5 years (30).

One study of *Wang et al.* demonstrated that MR findings contributed significant incremental value to the Partin tables in predicting OCPC. The contribution of MR findings was significant in all risk groups but was greatest in the intermediate- and high-risk groups. Overall, in the prediction of OCPC, the area under the ROC curve (AUC) for the staging nomograms was 0.80, while the AUC for

Table 1 Prostate tumor node metastasis (TNM) staging (American Joint Committee on Cancer, 7th ed. 2010)

<p>Evaluation of the (primary) tumor (T)</p> <p>Clinical</p> <p>TX: can not evaluate primary tumor</p> <p>T0: no evidence of primary tumor</p> <p>T1: clinically inapparent tumor neither palpable nor visible by imaging</p> <p>T1a: tumor was incidentally found in less than 5% of prostate tissue resected</p> <p>T1b: tumor was incidentally found in more than 5% of prostate tissue resected</p> <p>T1c: tumor was found in a needle biopsy performed because of elevated serum PSA</p> <p>T2: tumor confined within prostate¹</p> <p>T2a: the tumor is in half or less than half of one of the prostate gland's 2 lobes</p> <p>T2b: the tumor is in more than half of one lobe, but not both</p> <p>T2c: the tumor is in both lobes</p> <p>T3: the tumor has spread through the prostatic capsule (if it is only part-way through, it is still T2)</p> <p>T3a: the tumor has spread through the capsule on one or both sides</p> <p>T3b: the tumor has invaded one or both seminal vesicles</p> <p>T4: the tumor has invaded adjacent structures other than seminal vesicles (e.g. external sphincter, rectum, bladder, levator muscles, and/or pelvic wall)</p> <p>Pathologic (pT)²</p> <p>pT2: organ confined</p> <p>pT2a: unilateral, one-half of one side or less</p> <p>pT2b: unilateral, involving more than one-half of side but not both sides</p> <p>pT2c: bilateral disease</p> <p>pT3: extraprostatic extension</p> <p>pT3a: extraprostatic extension or microscopic invasion of bladder neck</p> <p>pT3b: seminal vesicles invasion</p> <p>pT4: Invasion of rectum, levator muscles, and/or pelvic wall</p>
<p>Evaluation of the regional lymph nodes (N)</p> <p>(p)NX: regional lymph nodes were not assessed (sampled)</p> <p>(p)N0: there has been no spread to the regional lymph nodes</p> <p>(p)N1: there has been spread to the regional lymph nodes</p>
<p>Evaluation of distant metastasis (M)</p> <p>M0: there is no distant metastasis</p> <p>M1: there is distant metastasis</p> <p>M1a: the cancer has spread to lymph nodes beyond the regional ones</p> <p>M1b: the cancer has spread to bone</p> <p>M1c: the cancer has spread to other sites (regardless of bone involvement)</p>
<p>¹Tumor found in one or both lobes by needle biopsy, but not palpable or reliably visible by imaging, is classified as T1c; ²There is no pathologic T1 classification</p>

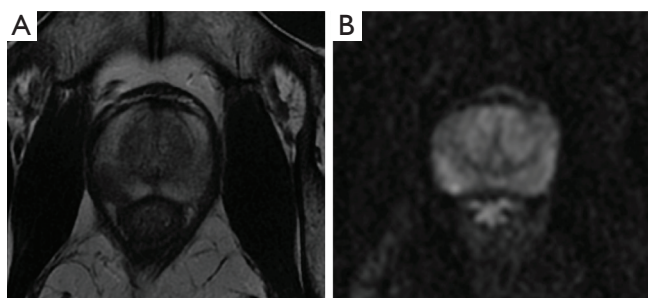


Figure 1 3T magnetic resonance (MR) images of organ-confined prostate cancer (OCPC) in a 59-year-old man with a Gleason score of 3+4 and a PSA level of 12.09 ng/mL. A. Transverse 3 mm-thick MR (4580/105) image shows a low-signal-intensity lesion in the right lobe of the prostate; B. Transverse 3 mm-thick DWI (3500/73, b-value of 1,000 s/mm²) clearly demonstrates a focal high intensity area, a finding indicative of increase diffusion

the staging nomograms plus MR findings was 0.88. In the combined endorectal MRI-MRSI group, the AUC were 0.81 for the staging nomograms and 0.90 for the staging nomograms plus MR findings (31).

Detection of extracapsular extension (ECE) (pT3a)

ECE of Pca is associated with increased risk of a positive surgical margin, which in turn influences postoperative biochemical recurrence after radical prostatectomy (32). On T2-weighted MRI, criteria for detecting ECE include at least one of the following: irregular capsular bulge or edge retraction, disruption of the prostatic capsule, extension into the periprostatic fat, broad contact with the capsule (>12 mm), obliteration of the rectoprostatic angle, or asymmetry of the neurovascular bundles (Figures 2,3) (33).

A study of 32 patients demonstrated the mean sensitivity, specificity, positive predictive value (PPV), and negative predictive value (NPV) for assessment of ECE with the combined DCE and T2WI 3 Tesla MRI system using an endorectal coil were 86%, 95%, 90%, and 93%, respectively (34). Bloch *et al.* (35) analysed the value of DCE combined with T2WI at 3 Tesla scanner for determining ECE of Pca, and found that the overall sensitivity, specificity, PPV and NPV for ECE were 75%, 92%, 79% and 91%, respectively. 3 Tesla MRI of the prostate combining DCE and T2WI is an accurate pretherapeutic staging tool for assessment of ECE in clinical practice. In a study using MRI with combining transaxial and coronal plane images using picture and communication systems (PACS) cross-referencing to

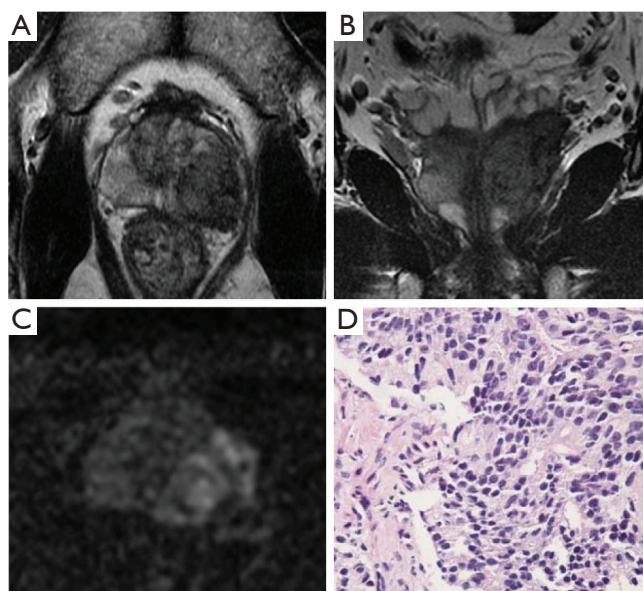


Figure 2 3T magnetic resonance (MR) images of extracapsular extension (ECE) of prostate cancer in a 57-year-old man with a Gleason score of 4+4 and a PSA level of 13.85 ng/mL. A and B. Transverse 3 mm-thick MR (4580/105) image, and coronal 3 mm-thick MR (2990/86) image show a hypointense tumor with extraprostatic extension in the left peripheral zone of the prostate; C. Transverse 3 mm-thick DWI (3500/73, b-value of 1,000 s/mm²) shows intense, increased signal (restricted diffusion) throughout the mass; D. The disease was clinically staged as T4 prostate cancer and confirmed by pathology

facilitate the diagnosis of ECE, Wang and colleagues (36) showed that sensitivity and specificity for ECE with MRI alone and with cross-referencing were 43% and 94% and 57% and 100% for reviewer 1 and 40% and 93% and 59% and 98% for reviewer 2, respectively. The weighted Kappa was 0.56 with MRI alone and 0.76 with cross-referencing, indicating good interobserver agreement.

Detection of seminal vesicle invasion (SVI) (pT3b)

SVI is considered an important marker of tumor progression and connected with increased risk of lymph node invasion, local tumor recurrence. On MRI T2WI direct signs of SVI are contiguous low-signal intensity (SI) tumor extension from base of the gland to seminal vesicles, focal low-SI within the seminal vesicles disruption or loss of the normal structure of the seminal vesicles, non-visualization or enlarged of the ejaculatory ducts, obliteration of seminal vesicle angle and decreased conspicuity of seminal vesicles (Figure 4).

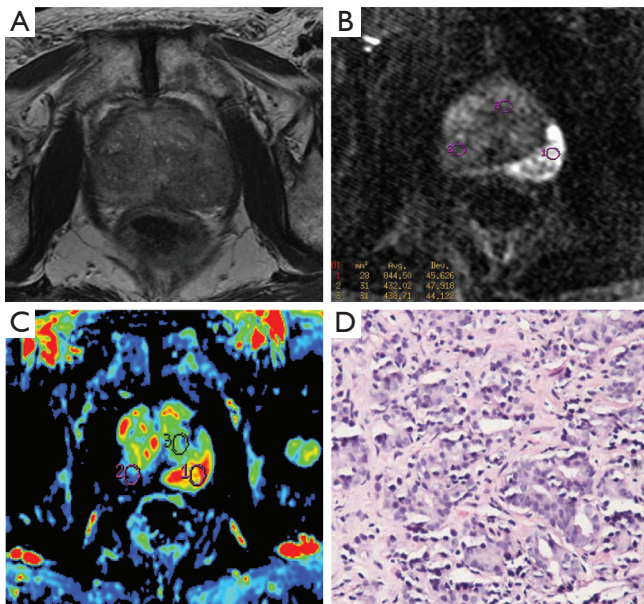


Figure 3 3T magnetic resonance (MR) images of extracapsular extension (ECE) of prostate cancer in a 69-year-old man with a Gleason score of 4+3 and a PSA level of 40.64 ng/mL. A. Transverse 3 mm-thick MR (4580/105) image shows a hypointense tumor with extraprostatic extension in the left peripheral zone of the prostate; B. Transverse 3 mm-thick DWI (3500/73, b-value of 1,000 s/mm²) shows intense, increased signal (restricted diffusion) throughout the mass; C. A color-coded wash-out map shows a focal area of wash-out in the location of cancer; D. The disease was clinically staged as T4 prostate cancer and confirmed by pathology

A study of 45 consecutive patients demonstrating the endorectal MRI following radiation therapy can help identify tumor sites and depict ECE and SVI with reasonable accuracy in patients with recurrent Pca (37). The AUC values for prediction of SVI were 0.76 (95% CI: 0.62, 0.90) for reader 1 and 0.70 (95% CI: 0.56, 0.85) for reader 2. The Kappa statistics used to assess interobserver agreement were fair (0.45, 0.47 for tumor location, SVI, respectively).

A study investigated 154 consecutive patients who underwent endorectal MRI before surgery. MRI sensitivity, specificity, PPV, NPV, overall accuracy resulted in respectively 0.88, 0.98, 0.82, 0.99 and 0.97 for SVI (38). Nepple *et al.* evaluated the accuracy of endorectal MRI compared with subsequent pathology specimen from prostatectomy. PPV, NPV, sensitivity, specificity of MRI were 93%, 75%, 94%, 38%, 99% for SVI. Endorectal MRI in the evaluation of high-risk Pca was moderately accurate

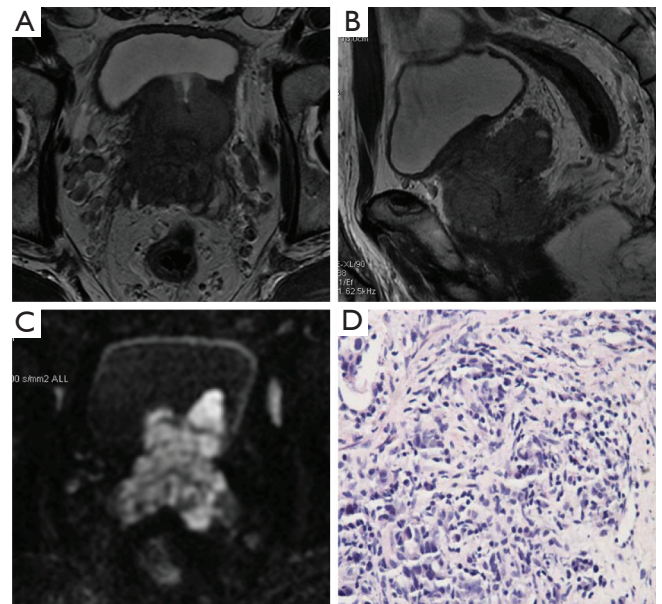


Figure 4 3T magnetic resonance (MR) images of seminal vesicle invasion (SVI) of prostate cancer in a 69-year-old man with a Gleason score of 4+4 and a PSA level of 49.7 ng/mL. A and B. Transverse 3 mm-thick MR (4580/105) image and sagittal 3 mm-thick MR (3088/70) image show a hypointense tumor with bilateral seminal vesicle invasion in the apex of the prostate; B. Transverse 3 mm-thick DWI (3500/73, b-value of 1,000 s/mm²) shows intense, increased signal (restricted diffusion) throughout the mass; D. The disease was clinically staged as T4 prostate cancer and confirmed by pathology

for SVI (39).

A study of 1,161 consecutive patients demonstrated that endorectal coil MRI had limited clinical value in preoperatively detecting SVI (40). In evaluating SVI, sensitivity and specificity were 33% and 89%, respectively. The PPV of MRI to assess SVI was 50% in both, with a NPV of 63%.

The addition of DWI to MRI has been shown to significantly increase staging accuracy for the less inexperienced readers and thus reduce interobserver variability (41). A study of 30 patients demonstrated significant improvement in the prediction of SVI for the less experienced readers. Interobserver agreement showed a substantial agreement (Kappa =0.613) for T2WI, and a substantial agreement (Kappa =0.737) for T2WI with DWI (41). In 2009, a study of Ren *et al.* showed that T2WI combined with DWI demonstrated significantly higher accuracy than T2WI alone in the detection of SVI (42).

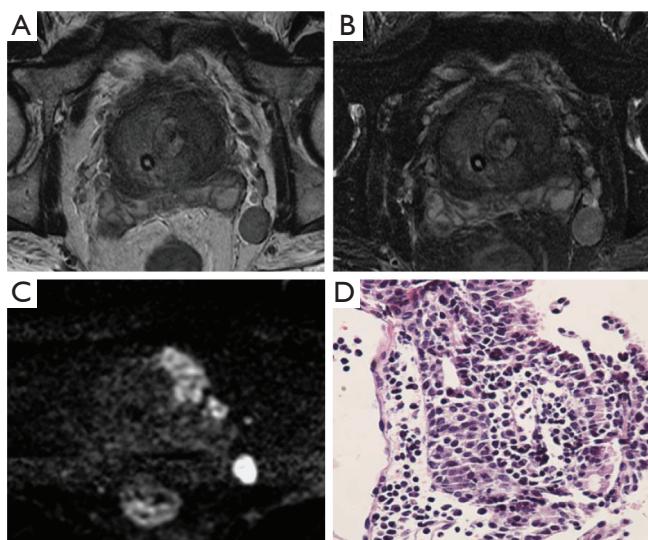


Figure 5 3T MR images of prostate cancer in a 72-year-old man with a Gleason score of 4+5 and a PSA level of 23.89 ng/mL. A and B. Transverse 3 mm-thick T2WI (4580/105) and transverse 3 mm-thick T2 weighted fat-saturated MR imaging (4580/105) show a hypointense tumor with extraprostatic extension in the left transitional and peripheral zone of the prostate, and intermediate SI bulky adenopathy with short-axis dimensions of >8 mm is present in left external iliac and obturator distributions; C. Transverse 3 mm-thick DWI (3500/73, b-value of 1,000 s/mm²) shows intense, increased signal (restricted diffusion) throughout the mass; D. The disease was clinically staged as T3M1 prostate cancer and confirmed by pathology

Detection of LNM

Regarding the lymph node metastasis (LNM), 70% of them are too small (<8 mm) to be evaluated using MRI, so conventional size criteria may underestimate the extent of nodal disease. A meta-analysis reported that MRI demonstrated equally poor performance in the detection of LNM from Pca with a sensitivity of around 30% (43). For this reason, recently two other MR techniques have been developed: MR lymphography (MRL) [which uses a lymph node-specific contrast agent called ultrasmall superparamagnetic particles of iron oxide (USPIO)] and DWI-MRI (Figure 5).

In 1998, Bellin *et al.* reported on the initial clinical experience with MRL and found a perfect sensitivity of 100% at 80% specificity (44). In another prospective study with 334 lymph nodes in 80 patients, sensitivity and specificity were 90.5% and 97.8%, respectively (45). More

recently, it has been shown that MRL is significantly more accurate than multidetector-row CT (46), and that in 41% of Pca patients MRL can detect LNM outside the surgical area of routine pelvic lymph node dissection (46). Although these results are very promising, MRL has not yet become available for clinical use due to the lack of an U.S. Food and Drug Administration (FDA)-approved lymph node-specific contrast agent.

The added value of DWI compared to USPIO-MRL did not improve diagnostic accuracy, but rather reduced significantly reading time for detecting pelvic LNM (47). However, one study also reported a good accuracy based on ADC value alone, with a sensitivity of 86.0% and a specificity of 85.3% (48).

A study of 411 consecutive patients demonstrated that MRI was an independent statistically significant predictor of LNM ($P=0.002$), with PPV and NPV value of 50% and 96.36%, respectively. On multivariate analysis, prediction of lymph node status using the model that included all MRI variables (ECE, SVI, and LNM) along with the Partin table results had also a significantly greater AUC than the univariate model that included only MRI LNM findings (AUC =0.892 *vs.* 0.633, respectively, $P<0.01$) (49).

Prostate cancer biologic potential

The Gleason scoring system remained one of the most powerful prognostic predictors in Pca for nearly 50 years after its initial description (50). It was endorsed as the primary staging system for Pca by the College of American Pathologists, the Armed Forces Institute of Pathology Fascicle on Prostate Cancer, the Association of Directors of Anatomic and Surgical Pathology, and the World Health Organization (WHO) (51).

Gleason grade has been associated with biochemical failure, local recurrences, and distant metastases such as skeletal and LNM after prostatectomy or radiation therapy (52-54). Since Gleason scores of 3+4, or lower, are associated with lower disease progression rates, and Gleason scores of 4+3, or higher, are associated with higher disease progression rates (55), a differentiating between both is meaningful.

Several studies reporting an association of Gleason staging with MRI are a great quantity, especially with DWI a significant negative correlation between Gleason score and ADC values been found (56,57). Furthermore, choline plus creatine-to-citrate ratios determined by using MRSI have also been correlated with Gleason grade (58,59). Wang *et al.*

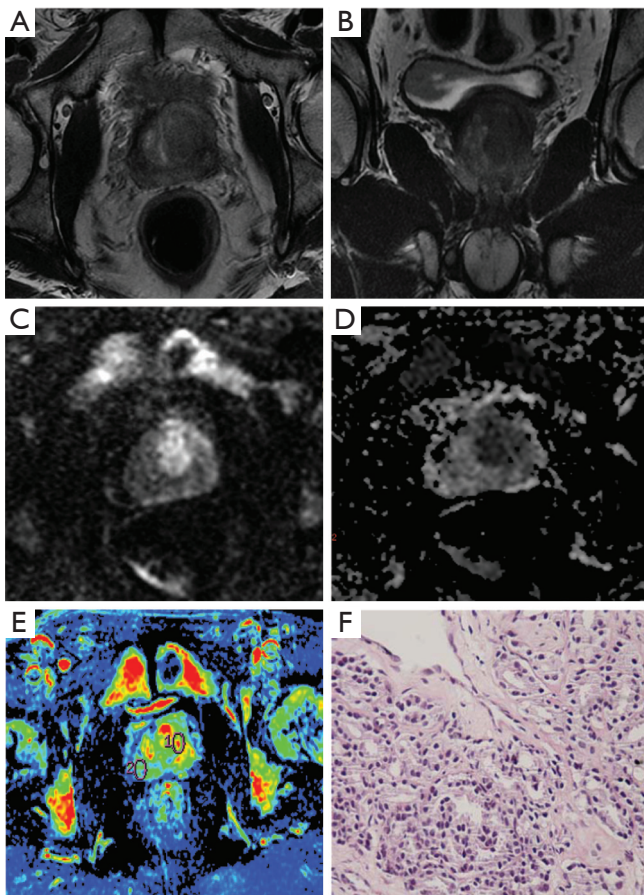


Figure 6 3T magnetic resonance (MR) images of extracapsular extension (ECE) of prostate cancer in a 56-year-old man with a Gleason score of 4+5 and a PSA level of 40.64 ng/mL. A and B. Transverse 3 mm-thick MR (4580/105) image and coronal 3 mm-thick MR (2990/86) image show a hypointense tumor with extraprostatic extension in the left transitional and peripheral zone of the prostate; C. Transverse 3 mm-thick DWI (3500/73, b-value of 1,000 s/mm²) shows intense, increased signal (restricted diffusion) throughout the mass; D. An ADC map shows a focal hypointense lesion extending outside the capsule; E. A color-coded wash-out map shows a focal area of wash-out in the location of cancer and left pulvic bone metastases; F. The disease was clinically staged as T3 prostate cancer and confirmed by pathology

even reported the correlation of SI of Pca on T2WI with Gleason grade and found that SI evaluation on T2WI may facilitate noninvasive assessment of Pca aggressiveness (60).

Treatment planning

There are several therapeutic options including pelvic

lymph node dissection (PLND), external beam radiotherapy (EBRT), radical prostatectomy (RP), androgen deprivation therapy (ADT), brachytherapy, cryosurgery, hyperthermia, and chemotherapy. Monotherapy or combination therapy is performed based on the TNM staging and clinical symptoms of the cancer. Good treatment strategies require a very careful evaluation of an individual prognosis to avoid inappropriate therapy induced morbidity or treatment failure. It is imperative that all tools available are used for different patients so that cancer is controlled.

RP is well established as a definitive treatment option in the management of localized Pca. The goal of this procedure is to achieve excellent oncologic control with negative surgical margins while preserving urinary continence and erectile function. A nerve-sparing radical prostatectomy preserves the neurovascular bundle (NVB) running along the posterior-lateral aspect of the prostate. This procedure is the standard of care for men with a low preoperative risk of extraprostatic diseases who wish to retain erectile function, and is also associated with improved urinary continence (61-64). The primary risk of nerve sparing is a positive surgical margin in a patient with organ-confined or extraprostatic extension (65,66). As such, accurate preoperative staging is very important for guiding treatment, and imaging techniques could provide a significant contribution.

Therapy response

Early selection of patients who are most likely to benefit from chemotherapy or radiotherapy may prevent the risk of toxicity in non-responding patients with prostate tumor. Early response to chemotherapy is monitored with DWI especially in bone metastases, as well as significant changes in perfusion due to tumor vascularity and extraction coefficient derived from DCE-MRI (Figure 6).

Foltz *et al.* found regional and temporal changes in ADC and T2 relaxation during radiation therapy (RT) in patients with low and intermediate risk localized Pca (67). A study of Franiel *et al.* showed statistically significant changes in perfusion and extraction coefficient parameters derived from DCE-MRI in monitoring the tissue changes to percutaneous intensity-modulated radiotherapy of Pca (68).

A study also demonstrated that after ADT, there was a significant reduction in all DCE-MRI parameters measured in tumor regions of interest (K^{trans} , K_{ep} , V_p). ADC values significantly decreased in areas of normal-appearing peripheral zone. As MRI provided dynamic information

that was helpful in therapy response, their findings suggested that DCE as a marker of angiogenesis may help demonstrate ADT resistance and DWI may be more accurate in determining presence of tumor cell death versus residual tumor (69).

Tumor recurrence

Approximately 25% to 30% of patients who underwent RP will develop local or systemic recurrent diseases (70,71). Biochemical failure (i.e., a rising serum PSA in the absence of demonstrable metastases) is widely accepted as an appropriate end point for defining treatment failure in men with localized Pca. The serum PSA is routinely used to monitor disease recurrence after definitive therapy because biochemical recurrence antedates metastatic disease progression and Pca-specific mortality by an average of 10 years, respectively (72-74). Biochemical recurrence-free probability after salvage radical prostatectomy at 5 years ranged from 37% to 55% and the estimated cancer-specific survival at 10 years ranged from 70% to 83% (75).

Diagnosis of recurrence of Pca remains challenging by imaging, especially in the early stage. At present, serial serum PSA test plays the important role in the assessment of recurrence and progression of Pca after initial radical treatment (76).

The current consensus considers a PSA increase over a threshold of 0.2 ng/mL as the cutoff that necessitates further evaluation (77). The main role of imaging would be to identify the patients with local recurrence who would potentially benefit from salvage radiotherapy. Detecting the site of recurrence is difficult, mainly because of the absence of any signs or symptoms in the early stage (78). A critical diagnostic dilemma for the evaluation of patients with biochemical failure is to differentiate between patients who only have local recurrence and those who have metastatic spread. At this point, diagnostic imaging strategies are able to provide crucial information toward differentiating local recurrence versus metastatic spread and in helping plan further therapeutic interventions.

To guide target biopsy for clinically suspected cancer in patients with negative biopsy Cancer suspicious regions (CSRs) seen on multiparametric MRI can be targeted for biopsy. This can be done by either performing a TRUS-guided biopsy or a MR-guided biopsy.

TRUS-guided prostate biopsy is the gold standard for the diagnosis of Pca. When applied as a sextant biopsy in patients with a total PSA value ranging from 4-10 ng/mL,

this approach has a sensitivity of 39-52% and a specificity of 81-82% (79). Yet, about 20% of Pca are not detected at the first biopsy. When the first biopsy is negative, a repeat biopsy may be recommended, which has a cancer detection rate between 20% to 35% (80-82).

MRI-guided prostate biopsy is a diagnostic option for patients with CSRs, this technology has gained growing importance in the diagnosis of Pca. The capability of combining MR imaging with techniques to simultaneously perform a targeted biopsy of the prostate is of particular interest to urologists.

Several studies have already demonstrated this technology improved cancerous detection rate in subjects with an elevated PSA and repetitive negative TRUS-guided biopsies (11,83,84). In a study of 54 patients with elevated PSA and negative biopsies, MRI had a sensitivity of 83% and a PPV of 50% for detection of Pca. A study of 92 patients concluded that for patients with elevated PSA and 2 previous negative biopsies, a negative MRI can rule out cancer and avoid subsequent biopsies (85).

In a study of 68 patients with repeat negative TRUS-guided prostate biopsies, the tumor detection rate of 3 Tesla MRI-guided biopsy was 59% (40 of 68 cases) using a median of 4 cores (86). In a study of 96 patients with TRUS-negative results, the sensitivity, specificity, PPV and NPV of MRI-guided core biopsies for Pca detection were 95.8%, 95.5%, 95.8% and 99.5% to 95.5% (87).

MR-compatible robots for transrectal prostate biopsy are being developed. Preliminary results found in phantom and patient feasibility studies are promising (88-90). In future studies, robotics could also play an important role in guiding focal treatment of PCa. But before robot-assisted MRI guided focal therapy can be realized, further extensive research needs to be done.

Future prospects

Although functional MR system for staging Pca on 1.5 Tesla is commercially available and is becoming more widely used, 3 Tesla MR scanners offer improvements in both spatial and temporal resolution and in speed. Increasing static magnetic field strength, B_0 , from 1.5 Tesla to 3 Tesla will result in a theoretical doubling of the signal-to-noise ratio (SNR). The increase in SNR results in an increase in spatial and temporal resolution and a decrease in the acquisition time (91). However, a disadvantage of 3 Tesla is the increased susceptibility effect in comparison with 1.5 Tesla due to the higher field inhomogeneity as

well as the chemical shift effect, which are directly related to magnetic field strength (92).

Conclusions

The increasing incidence of Pca, which is the most frequently diagnosed malignancy in the Western male population (1), poses an increasing burden on health care. MRI is able to provide detailed anatomical images due to high spatial resolution, superior contrast resolution and multiplanar capability (93). MRI noninvasively improves cancer staging, biologic potential and treatment planning, monitors antitumor therapy and local recurrence, and guides target biopsy for clinically suspected cancer with previous negative biopsy. State-of-the-art techniques, such as DWI, MRSI, DCE-MRI, high-field strength scanner, image postprocessing and PACS improved interpretation of Pca images. To interpret these studies accurately, there is still a need for multi-institutional studies to standardize functional MRI techniques and interpretation criteria.

Acknowledgements

The work described in this paper was supported by a grant from the National Natural Science Foundation of China (Project No. 81171307).

Disclosure: The authors declare no conflict of interest.

References

1. Siegel R, Naishadham D, Jemal A. Cancer statistics, 2013. *CA Cancer J Clin* 2013;63:11-30.
2. Jemal A, Center MM, DeSantis C, et al. Global patterns of cancer incidence and mortality rates and trends. *Cancer Epidemiol Biomarkers Prev* 2010;19:1893-907.
3. Ferlay J, Autier P, Boniol M, et al. Estimates of the cancer incidence and mortality in Europe in 2006. *Ann Oncol* 2007;18:581-92.
4. Hankey BF, Feuer EJ, Clegg LX, et al. Cancer surveillance series: interpreting trends in prostate cancer--part I: Evidence of the effects of screening in recent prostate cancer incidence, mortality, and survival rates. *J Natl Cancer Inst* 1999;91:1017-24.
5. Moyer VA, U.S. Preventive Services Task Force. Screening for prostate cancer: U.S. Preventive Services Task Force recommendation statement. *Ann Intern Med* 2012;157:120-34.
6. Fine SW, Amin MB, Berney DM, et al. A contemporary update on pathology reporting for prostate cancer: biopsy and radical prostatectomy specimens. *Eur Urol* 2012;62:20-39.
7. Kälkner KM, Wahlgren T, Ryberg M, et al. Clinical outcome in patients with prostate cancer treated with external beam radiotherapy and high dose-rate iridium 192 brachytherapy boost: a 6-year follow-up. *Acta Oncol* 2007;46:909-17.
8. Fütterer JJ. MR imaging in local staging of prostate cancer. *Eur J Radiol* 2007;63:328-34.
9. Hoeks CM, Barentsz JO, Hambrock T, et al. Prostate cancer: multiparametric MR imaging for detection, localization, and staging. *Radiology* 2011;261:46-66.
10. Colleselli D, Hennenlotter J, Schilling D, et al. Impact of clinical parameters on the diagnostic accuracy of endorectal coil MRI for the detection of prostate cancer. *Urol Int* 2011;86:393-8.
11. Hambrock T, Fütterer JJ, Huisman HJ, et al. Thirty-two-channel coil 3T magnetic resonance-guided biopsies of prostate tumor suspicious regions identified on multimodality 3T magnetic resonance imaging: technique and feasibility. *Invest Radiol* 2008;43:686-94.
12. Franiel T, Lüdemann L, Rudolph B, et al. Evaluation of normal prostate tissue, chronic prostatitis, and prostate cancer by quantitative perfusion analysis using a dynamic contrast-enhanced inversion-prepared dual-contrast gradient echo sequence. *Invest Radiol* 2008;43:481-7.
13. Tan CH, Wei W, Johnson V, et al. Diffusion-weighted MRI in the detection of prostate cancer: meta-analysis. *AJR Am J Roentgenol* 2012;199:822-9.
14. Wu LM, Xu JR, Gu HY, et al. Usefulness of diffusion-weighted magnetic resonance imaging in the diagnosis of prostate cancer. *Acad Radiol* 2012;19:1215-24.
15. Morgan VA, Riches SF, Giles S, et al. Diffusion-weighted MRI for locally recurrent prostate cancer after external beam radiotherapy. *AJR Am J Roentgenol* 2012;198:596-602.
16. Heijmink SW, Scheenen TW, Fütterer JJ, et al. Prostate and lymph node proton magnetic resonance (MR) spectroscopic imaging with external array coils at 3 T to detect recurrent prostate cancer after radiation therapy. *Invest Radiol* 2007;42:420-7.
17. Caivano R, Cirillo P, Balestra A, et al. Prostate cancer in magnetic resonance imaging: diagnostic utilities of spectroscopic sequences. *J Med Imaging Radiat Oncol* 2012;56:606-16.
18. Vilanova JC, Barceló-Vidal C, Comet J, et al. Usefulness of prebiopsy multifunctional and morphologic MRI

- combined with free-to-total prostate-specific antigen ratio in the detection of prostate cancer. *AJR Am J Roentgenol* 2011;196:W715-22.
19. Rischke HC, Schäfer AO, Nestle U, et al. Detection of local recurrent prostate cancer after radical prostatectomy in terms of salvage radiotherapy using dynamic contrast enhanced-MRI without endorectal coil. *Radiat Oncol* 2012;7:185.
 20. Chen YJ, Chu WC, Pu YS, et al. Washout gradient in dynamic contrast-enhanced MRI is associated with tumor aggressiveness of prostate cancer. *J Magn Reson Imaging* 2012;36:912-9.
 21. Verma S, Turkbey B, Muradyan N, et al. Overview of dynamic contrast-enhanced MRI in prostate cancer diagnosis and management. *AJR Am J Roentgenol* 2012;198:1277-88.
 22. Zelfhof B, Lowry M, Rodrigues G, et al. Description of magnetic resonance imaging-derived enhancement variables in pathologically confirmed prostate cancer and normal peripheral zone regions. *BJU Int* 2009;104:621-7.
 23. Wu LM, Xu JR, Ye YQ, et al. The clinical value of diffusion-weighted imaging in combination with T2-weighted imaging in diagnosing prostate carcinoma: a systematic review and meta-analysis. *AJR Am J Roentgenol* 2012;199:103-10.
 24. Mueller-Lisse UG, Scherr MK. Proton MR spectroscopy of the prostate. *Eur J Radiol* 2007;63:351-60.
 25. Shukla-Dave A, Hricak H, Moskowitz C, et al. Detection of prostate cancer with MR spectroscopic imaging: an expanded paradigm incorporating polyamines. *Radiology* 2007;245:499-506.
 26. Wang L, Van den Bos IC, Hussain SM, et al. Post-processing of dynamic gadolinium-enhanced magnetic resonance imaging exams of the liver: explanation and potential clinical applications for color-coded qualitative and quantitative analysis. *Acta Radiol* 2008;49:6-18.
 27. Edge SB, Byrd DR, Compton CC, et al. eds. *AJCC cancer staging manual*. 7th ed. New York: Springer-Verlag, 2010.
 28. Presti JC Jr. Prostate cancer: assessment of risk using digital rectal examination, tumor grade, prostate-specific antigen, and systematic biopsy. *Radiol Clin North Am* 2000;38:49-58.
 29. Scardino PT. Continuing refinements in radical prostatectomy: more evidence that technique matters. *J Urol* 2005;173:338-9.
 30. Ohori M, Kattan MW, Koh H, et al. Predicting the presence and side of extracapsular extension: a nomogram for staging prostate cancer. *J Urol* 2004;171:1844-9; discussion 1849.
 31. Wang L, Hricak H, Kattan MW, et al. Prediction of organ-confined prostate cancer: incremental value of MR imaging and MR spectroscopic imaging to staging nomograms. *Radiology* 2006;238:597-603.
 32. Godoy G, Tareen BU, Lepor H. Site of positive surgical margins influences biochemical recurrence after radical prostatectomy. *BJU Int* 2009;104:1610-4.
 33. Wang L, Mullerad M, Chen HN, et al. Prostate cancer: incremental value of endorectal MR imaging findings for prediction of extracapsular extension. *Radiology* 2004;232:133-9.
 34. Bloch BN, Furman-Haran E, Helbich TH, et al. Prostate cancer: accurate determination of extracapsular extension with high-spatial-resolution dynamic contrast-enhanced and T2-weighted MR imaging--initial results. *Radiology* 2007;245:176-85.
 35. Bloch BN, Genega EM, Costa DN, et al. Prediction of prostate cancer extracapsular extension with high spatial resolution dynamic contrast-enhanced 3-T MRI. *Eur Radiol* 2012;22:2201-10.
 36. Wang L, Zhang J, Schwartz LH, et al. Incremental value of multiplanar cross-referencing for prostate cancer staging with endorectal MRI. *AJR Am J Roentgenol* 2007;188:99-104.
 37. Sala E, Eberhardt SC, Akin O, et al. Endorectal MR imaging before salvage prostatectomy: tumor localization and staging. *Radiology* 2006;238:176-83.
 38. Porcaro AB, Borsato A, Romano M, et al. Accuracy of preoperative endo-rectal coil magnetic resonance imaging in detecting clinical under-staging of localized prostate cancer. *World J Urol* 2012;30:1-7.
 39. Nepple KG, Rosevear HM, Stolpen AH, et al. Concordance of preoperative prostate endorectal MRI with subsequent prostatectomy specimen in high-risk prostate cancer patients. *Urol Oncol* 2011. [Epub ahead of print].
 40. Brajtford JS, Lavery HJ, Nabizada-Pace F, et al. Endorectal magnetic resonance imaging has limited clinical ability to preoperatively predict pT3 prostate cancer. *BJU Int* 2011;107:1419-24.
 41. Kim CK, Choi D, Park BK, et al. Diffusion-weighted MR imaging for the evaluation of seminal vesicle invasion in prostate cancer: initial results. *J Magn Reson Imaging* 2008;28:963-9.
 42. Ren J, Huan Y, Wang H, et al. Seminal vesicle invasion in prostate cancer: prediction with combined T2-weighted and diffusion-weighted MR imaging. *Eur Radiol*

- 2009;19:2481-6.
43. Hövels AM, Heesakkers RA, Adang EM, et al. The diagnostic accuracy of CT and MRI in the staging of pelvic lymph nodes in patients with prostate cancer: a meta-analysis. *Clin Radiol* 2008;63:387-95.
 44. Bellin MF, Roy C, Kinkel K, et al. Lymph node metastases: safety and effectiveness of MR imaging with ultrasmall superparamagnetic iron oxide particles--initial clinical experience. *Radiology* 1998;207:799-808.
 45. Harisinghani MG, Barentsz J, Hahn PF, et al. Noninvasive detection of clinically occult lymph-node metastases in prostate cancer. *N Engl J Med* 2003;348:2491-9.
 46. Heesakkers RA, Jager GJ, Hövels AM, et al. Prostate cancer: detection of lymph node metastases outside the routine surgical area with ferumoxtran-10-enhanced MR imaging. *Radiology* 2009;251:408-14.
 47. Thoeny HC, Triantafyllou M, Birkhaeuser FD, et al. Combined ultrasmall superparamagnetic particles of iron oxide-enhanced and diffusion-weighted magnetic resonance imaging reliably detect pelvic lymph node metastases in normal-sized nodes of bladder and prostate cancer patients. *Eur Urol* 2009;55:761-9.
 48. Eiber M, Beer AJ, Holzapfel K, et al. Preliminary results for characterization of pelvic lymph nodes in patients with prostate cancer by diffusion-weighted MR-imaging. *Invest Radiol* 2010;45:15-23.
 49. Wang L, Hricak H, Kattan MW, et al. Combined endorectal and phased-array MRI in the prediction of pelvic lymph node metastasis in prostate cancer. *AJR Am J Roentgenol* 2006;186:743-8.
 50. Epstein JI. An update of the Gleason grading system. *J Urol* 2010;183:433-40.
 51. Epstein JI, Algaba F, Allsbrook WC Jr, et al. WHO classification of tumours: Pathology and genetics of tumours of the urinary system and male genital organs. Lyon: IARC Press, 2004:179-84.
 52. Babaian RJ, Troncso P, Bhadkamkar VA, et al. Analysis of clinicopathologic factors predicting outcome after radical prostatectomy. *Cancer* 2001;91:1414-22.
 53. Bruns F, Franzki C, Wegener G, et al. Definitive conformal radiotherapy for localized high-risk prostate cancer: a long-term follow-up study with PSA course. *Anticancer Res* 2007;27:1847-51.
 54. Kattan MW, Zelefsky MJ, Kupelian PA, et al. Pretreatment nomogram that predicts 5-year probability of metastasis following three-dimensional conformal radiation therapy for localized prostate cancer. *J Clin Oncol* 2003;21:4568-71.
 55. Chan TY, Partin AW, Walsh PC, et al. Prognostic significance of Gleason score 3+4 versus Gleason score 4+3 tumor at radical prostatectomy. *Urology* 2000;56:823-7.
 56. Litjens GJ, Hambrock T, Hulsbergen-van de Kaa C, et al. Interpatient variation in normal peripheral zone apparent diffusion coefficient: effect on the prediction of prostate cancer aggressiveness. *Radiology* 2012;265:260-6.
 57. Turkbey B, Shah VP, Pang Y, et al. Is apparent diffusion coefficient associated with clinical risk scores for prostate cancers that are visible on 3-T MR images? *Radiology* 2011;258:488-95.
 58. Klijn S, De Visschere PJ, De Meerleer GO, et al. Comparison of qualitative and quantitative approach to prostate MR spectroscopy in peripheral zone cancer detection. *Eur J Radiol* 2012;81:411-6.
 59. Westphalen AC, Coakley FV, Qayyum A, et al. Peripheral zone prostate cancer: accuracy of different interpretative approaches with MR and MR spectroscopic imaging. *Radiology* 2008;246:177-84.
 60. Wang L, Mazaheri Y, Zhang J, et al. Assessment of biologic aggressiveness of prostate cancer: correlation of MR signal intensity with Gleason grade after radical prostatectomy. *Radiology* 2008;246:168-76.
 61. Oefelein MG. Prospective predictors of urinary continence after anatomical radical retropubic prostatectomy: a multivariate analysis. *World J Urol* 2004;22:267-71.
 62. Burkhard FC, Kessler TM, Fleischmann A, et al. Nerve sparing open radical retropubic prostatectomy--does it have an impact on urinary continence? *J Urol* 2006;176:189-95.
 63. Dubbelman YD, Dohle GR, Schröder FH. Sexual function before and after radical retropubic prostatectomy: A systematic review of prognostic indicators for a successful outcome. *Eur Urol* 2006;50:711-8; discussion 718-20.
 64. Walz J, Burnett AL, Costello AJ, et al. A critical analysis of the current knowledge of surgical anatomy related to optimization of cancer control and preservation of continence and erection in candidates for radical prostatectomy. *Eur Urol* 2010;57:179-92.
 65. Hull GW, Rabbani F, Abbas F, et al. Cancer control with radical prostatectomy alone in 1,000 consecutive patients. *J Urol* 2002;167:528-34.
 66. Grossfeld GD, Chang JJ, Broering JM, et al. Under staging and under grading in a contemporary series of patients undergoing radical prostatectomy: results from the Cancer of the Prostate Strategic Urologic Research Endeavor database. *J Urol* 2001;165:851-6.
 67. Foltz WD, Wu A, Chung P, et al. Changes in apparent

- diffusion coefficient and T(2) relaxation during radiotherapy for prostate cancer. *J Magn Reson Imaging* 2013;37:909-16.
68. Franiel T, Lüdemann L, Taupitz M, et al. MRI before and after external beam intensity-modulated radiotherapy of patients with prostate cancer: the feasibility of monitoring of radiation-induced tissue changes using a dynamic contrast-enhanced inversion-prepared dual-contrast gradient echo sequence. *Radiother Oncol* 2009;93:241-5.
 69. Barrett T, Gill AB, Kataoka MY, et al. DCE and DW MRI in monitoring response to androgen deprivation therapy in patients with prostate cancer: a feasibility study. *Magn Reson Med* 2012;67:778-85.
 70. Djavan B, Moul JW, Zlotta A, et al. PSA progression following radical prostatectomy and radiation therapy: new standards in the new Millennium. *Eur Urol* 2003;43:12-27.
 71. Khan MA, Han M, Partin AW, et al. Long-term cancer control of radical prostatectomy in men younger than 50 years of age: update 2003. *Urology* 2003;62:86-91; discussion 91-2.
 72. Stephenson AJ, Kattan MW, Eastham JA, et al. Prostate cancer-specific mortality after radical prostatectomy for patients treated in the prostate-specific antigen era. *J Clin Oncol* 2009;27:4300-5.
 73. Freedland SJ, Humphreys EB, Mangold LA, et al. Risk of prostate cancer-specific mortality following biochemical recurrence after radical prostatectomy. *JAMA* 2005;294:433-9.
 74. Freedland SJ, Humphreys EB, Mangold LA, et al. Time to prostate specific antigen recurrence after radical prostatectomy and risk of prostate cancer specific mortality. *J Urol* 2006;176:1404-8.
 75. Rosoff JS, Savage SJ, Prasad SM. Salvage radical prostatectomy as management of locally recurrent prostate cancer: outcomes and complications. *World J Urol* 2013. [Epub ahead of print].
 76. Sakai I, Harada K, Kurahashi T, et al. Usefulness of the nadir value of serum prostate-specific antigen measured by an ultrasensitive assay as a predictor of biochemical recurrence after radical prostatectomy for clinically localized prostate cancer. *Urol Int* 2006;76:227-31.
 77. Heidenreich A, Aus G, Bolla M, et al. EAU guidelines on prostate cancer. *Eur Urol* 2008;53:68-80.
 78. Tamsel S, Killi R, Apaydin E, et al. The potential value of power Doppler ultrasound imaging compared with grey-scale ultrasound findings in the diagnosis of local recurrence after radical prostatectomy. *Clin Radiol* 2006;61:325-30; discussion 323-4.
 79. Heijmink SW, van Moerkerk H, Kiemeny LA, et al. A comparison of the diagnostic performance of systematic versus ultrasound-guided biopsies of prostate cancer. *Eur Radiol* 2006;16:927-38.
 80. Postma R, Roobol M, Schröder FH, et al. Lesions predictive for prostate cancer in a screened population: first and second screening round findings. *Prostate* 2004;61:260-6.
 81. Zaytoun OM, Stephenson AJ, Fareed K, et al. When serial prostate biopsy is recommended: most cancers detected are clinically insignificant. *BJU Int* 2012;110:987-92.
 82. Djavan B, Ravery V, Zlotta A, et al. Prospective evaluation of prostate cancer detected on biopsies 1, 2, 3 and 4: when should we stop? *J Urol* 2001;166:1679-83.
 83. Anastasiadis AG, Lichy MP, Nagele U, et al. MRI-guided biopsy of the prostate increases diagnostic performance in men with elevated or increasing PSA levels after previous negative TRUS biopsies. *Eur Urol* 2006;50:738-48; discussion 748-9.
 84. Beyersdorff D, Taupitz M, Winkelmann B, et al. Patients with a history of elevated prostate-specific antigen levels and negative transrectal US-guided quadrant or sextant biopsy results: value of MR imaging. *Radiology* 2002;224:701-6.
 85. Comet-Battle J, Vilanova-Busquets JC, Saladié-Roig JM, et al. The value of endorectal MRI in the early diagnosis of prostate cancer. *Eur Urol* 2003;44:201-7; discussion 207-8.
 86. Hambrock T, Somford DM, Hoeks C, et al. Magnetic resonance imaging guided prostate biopsy in men with repeat negative biopsies and increased prostate specific antigen. *J Urol* 2010;183:520-7.
 87. Engehausen DG, Engelhard K, Schwab SA, et al. Magnetic resonance image-guided biopsies with a high detection rate of prostate cancer. *ScientificWorldJournal* 2012;2012:975971.
 88. van den Bosch MR, Moman MR, van Vulpen M, et al. MRI-guided robotic system for transperineal prostate interventions: proof of principle. *Phys Med Biol* 2010;55:N133-40.
 89. Fischer GS, Iordachita I, Csoma C, et al. MRI-Compatible Pneumatic Robot for Transperineal Prostate Needle Placement. *IEEE ASME Trans Mechatron* 2008;13:295-305.
 90. Yakar D, Schouten MG, Bosboom DG, et al. Feasibility of a pneumatically actuated MR-compatible robot for transrectal prostate biopsy guidance. *Radiology* 2011;260:241-7.

91. Barth MM, Smith MP, Pedrosa I, et al. Body MR imaging at 3.0 T: understanding the opportunities and challenges. *Radiographics* 2007;27:1445-62; discussion 1462-4.
92. Chang KJ, Kamel IR, Macura KJ, et al. 3.0-T MR imaging of the abdomen: comparison with 1.5 T. *Radiographics* 2008;28:1983-98.
93. Claus FG, Hricak H, Hattery RR. Pretreatment evaluation of prostate cancer: role of MR imaging and 1H MR spectroscopy. *Radiographics* 2004;24:S167-80.

Cite this article as: Li L, Wang L, Feng Z, Hu Z, Wang G, Yuan X, Wang H, Hu D. Prostate cancer magnetic resonance imaging (MRI): multidisciplinary standpoint. *Quant Imaging Med Surg* 2013;3(2):100-112. doi: 10.3978/j.issn.2223-4292.2013.03.03